THE JOURNAL OF PHYSICAL CHEMISTRY A

Article

Cite This: J. Phys. Chem. A 2019, 123, 9193−9198

pubs.acs.org/JPCA

Threshold Photoelectron Spectrum of the Anilino Radical

Helgi Rafn Hrodmarsson,*[,†,#] Gustavo A. Garcia,[†] Laurent Nahon,[†] Bérenger Gans,[‡] and Jean-Christophe Loison[§]

[†]Synchrotron SOLEIL, L'Orme des Merisiers, St Aubin, BP 48, 91192 Gif sur Yvette, France

[‡]Institut des Sciences Moléculaires d'Orsay (ISMO), UMR 8214 CNRS, Univ. Paris-Sud, Université Paris-Saclay, F-91405 Orsay Cedex, France

[§]Institut des Sciences Moléculaires (ISM), CNRS, Univ. Bordeaux, 351 cours de la Libération, 33400 Talence, France

Supporting Information

ABSTRACT: We report on the photoionization of the resonance-stabilized anilino radical (C_6H_5NH) formed by H atom abstraction from aniline by F atoms in a flow tube. The spectra were recorded from 7.8 to 9.7 eV by using a double-imaging photoelectron/photoion coincidence spectrometer with VUV radiation provided by the DESIRS beamline at the SOLEIL synchrotron. The vibrationally resolved recorded threshold photoelectron spectrum of the anilino radical showed transitions to the ground $X^{+1}A' \leftarrow X^2A''$ and first excited states $a^{+3}A'' \leftarrow X^2A''$ of the cation, which were assigned through comparison with theoretically simulated spectra, yielding an adiabatic ionization energy of 8.02 ± 0.02 eV. These results are discussed in light of existing data on the picolyl structural isomers and are of interest for the analytical applications of coincidence techniques in real-time combustion analysis where these intermediates are found.

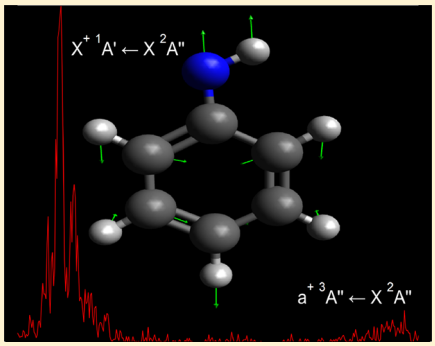

INTRODUCTION

Aniline (or aminobenzene) is the epitome of a prototypical aromatic amine and is of fundamental interest in terms of understanding photodissociation dynamics via $1\pi\sigma^*$ states localized at amino moieties in complex heteroaromatic species.[1] It has been shown that N−H bond fission in heteroatom molecules is not only prompt[2] but also an important contributor to nonradiative decay of heteroaromatics.[3] The study of such nitrogen-containing aromatics in terms of their photostability and characteristics is thus axiomatically of importance in biophysics,[4] and they have been attracting interest recently due to their role as reactive intermediates in biofuel combustion,[5] coal pyrolysis,[6] and astrochemistry.[7]

Aniline photodissociates to produce the anilino radical (C_6H_5NH) and a H photofragment via the $1\pi\sigma^*$ state,[8] which is energetically accessible at 269.513 nm (4.600 eV). The most recent experimental and theoretical efforts into studying these photodissociation dynamics of aniline have recently been succinctly summarized.[4] The anilino radical (see Figure 1) also appears as a reaction intermediate in the reaction between $N(^2D)$ atoms and benzene, which is of interest to chemistry in the Titan's atmosphere.[9,10] Despite the anilino radical itself appearing as a photoproduct in multiple studies of the dissociation of its parent molecule, aniline, it has been very modestly studied,[8,11−18] and in particular, to our knowledge, no photoelectron spectrum (PES) of the neutral anilino radical has ever been reported.

Apart from the neutral and cationic structural information that can be extracted by comparing experimental and theoretical photoelectron spectra, in recent years, there have been successful applications of advanced mass spectrometric methods based on imaging photoelectron/photoion coincidence (i^2PEPICO) techniques,[19] coupled to synchrotron

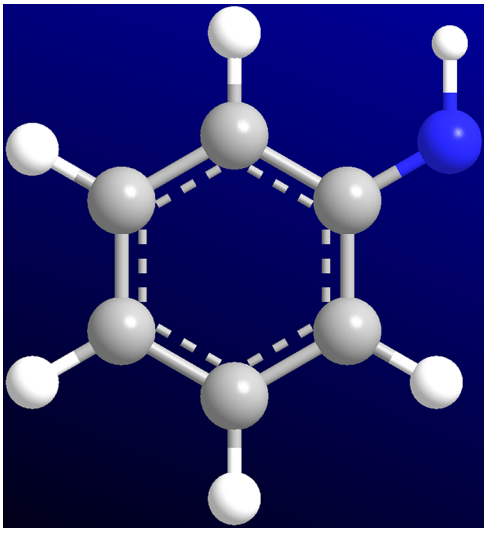

Figure 1. Molecular structure of the anilino radical C_6H_5NH. Carbon atoms, hydrogen atoms, and nitrogen are shown in gray, white, and blue, respectively.

Received: July 30, 2019
Revised: September 12, 2019
Published: September 26, 2019

DOI: 10.1021/acs.jpca.9b07273
J. Phys. Chem. A 2019, 123, 9193−9198

radiation, for the study of complex chemical reactions in the gas phase. Through these coincidence schemes, the photoelectron spectrum, recorded by dispersing the energies of either the photons or the electrons,[20] correlated to any peak in the time-of-flight mass spectrum can be extracted in a highly multiplex manner. Because isomers are expected to possess different vibronic structures, the photoelectron spectrum can, in principle, be used as a molecular fingerprint, and this has been applied to not only in real-time, in situ species identification, especially in the combustion community,[20−24] but also in other types of complex chemical analyses.[25,26] In this context, obtaining the anilino radical photoelectron fingerprint is of interest because resonantly stabilized radicals containing nitrogen can be found in both the combustion chemistry and Titan's atmosphere.

Even more interesting is the fact that three additional structural isomers (C_6H_6N), namely, 2-picolyl, 3-picolyl, and 4-picolyl, were recently studied in this context and their coincidence threshold photoelectron spectra were recorded.[27] All of these picolyl radicals have very similar spectral appearances, but each has a distinct ionization onset, thus making them easily identifiable.

Here, we present the first threshold photoelectron spectrum (TPES) of the ground state and first excited state of the cation of the anilino radical as well as the first measurement of the radical's adiabatic ionization potential. We also compare the anilino TPES to those of its picolyl isomers and discuss potential issues related to disentangling the spectra of these structural isomers.

METHODS

Experimental. Experiments were performed on the DESIRS VUV undulator beamline[28] located at the third-generation French national synchrotron facility SOLEIL (Gif-sur-Yvette, France). Aniline was obtained commercially (Sigma-Aldritch, ≥98% purity), and the anilino radical was obtained via the reaction

$$C_6H_5NH_2 + F \rightarrow C_6H_5NH + HF$$

where F atoms were produced from a 5% F_2/He mixture in a microwave discharge and injected into a flow tube reactor[29] placed inside the permanent molecular beam end-station SAPHIRS,[30] while the aniline was highly diluted in He and added through a movable injector. The distance between the injector and skimmer determines the reaction time, typically around 1 ms. The total pressure in the reactor was regulated at 1 torr, and the concentrations of F and $C_6H_5NH_2$ were estimated at 5.0×10^{13} atoms/cm^3 and 1.0×10^{15} molecules/cm^3, respectively.

The monochromator was set to deliver a photon energy resolution of 3 meV at 8 eV. A gas filter upstream of the beamline monochromator was filled with krypton to filter out the higher harmonics from the undulator, which might be transmitted by the high orders of the monochromator's grating. We used very weak residual harmonics to our advantage by calibrating the energy scale with the ionization of helium, which is achieved by the third harmonic of the undulator at 8.1957 eV. It should be noted that the higher harmonics from the undulator are almost completely quenched (by 4−5 orders of magnitude) and do not impact our results. The appearance of He ionization via the third harmonic coming from the undulator is a testament to the abundance of He in the beam as it was the designated carrier gas for aniline and F_2 and was thus, by far, the largest component in the molecular beam, but its observed weak signal is not problematic for the data analysis owing to the PEPICO mass-tagging scheme.

The i^{2}PEPICO spectrometer DELICIOUS3[31] was used to detect electrons and ions in coincidence with a velocity map imaging (VMI) setup and an imaging linear time-of-flight analyzer, respectively. Particle acceleration was achieved with a DC field of 53 V cm^{-1}, which leads to a lowering of the ionization threshold by ∼5 meV. This shift is accounted for in the energy scale calibration. Through the coincidence scheme, mass-selected photoelectron images correlated to the anilino radical (m/z 92) having a net velocity along the molecular beam direction, as selected by defining a region of interest in the coincident ion images, were recorded in the 7.8−9.7 eV range with 5 meV steps. Following inversion of these images,[32] the electron signal detected in coincidence with anilino ions is obtained as a function of electron kinetic energy and photon energy. In such a two-dimensional (2D) matrix, oblique diagonal lines correspond to direct ionization to a cationic state, where the kinetic energy of the produced photoelectrons increases linearly with the excess energy, $h\nu - \mathrm{IE}_i$, IE_i being the ionization energy of the ith state. The threshold photoelectron spectrum, or TPES, is obtained by integrating the pixel intensities along these diagonal lines up to a relatively small value of kinetic energy according to

$$\mathrm{TPES}(h\nu) = \int_0^{KE_{\max}} A(h\nu + KE, \mathrm{KE})\mathrm{d}KE$$

where A is the two-dimensional intensity matrix representing the number of coincident events as a function of photon and electron kinetic energy, and $\mathrm{KE}_{\max}$ is the maximum kinetic energy, here, 75 meV, which resulted in a full TPES resolution of 20 meV, as derived from the third-order ionization of He.

This method offers a better compromise between the resolution and signal intensity when compared with how the TPES is traditionally obtained[19] since more energetic electrons can be taken into account without degrading the resolution. This is useful in this particular case because the energy range of interest lies above the ionization of the parent precursor, aniline ($C_6H_5NH_2$), at 7.720 eV,[33] which by far dominates the mass spectrum (see Figure S1), lowering the signal-to-noise ratio on the anilino signal. An additional and sometimes valuable effect is the enhanced sensitivity to autoionizations.[34] This also implies that the method described above can show a very poor agreement with theoretical Franck−Condon (FC) factors if on-resonance autoionizations are encountered when $\mathrm{KE}_{\max}$ is increased. To this end, a traditionally obtained TPES would be better suitable to provide better (although not perfect) fits to simulated FC factors but ultimately with a poorer signal-to-noise ratio.

Theoretical. The electronic structure calculations for the geometry optimization and harmonic frequencies calculations of both the neutral and the cation were carried out at the DFT level (M06-2X) using the AVTZ basis set with Gaussian09.[35] The adiabatic energy was obtained as the difference between their energies after correction by their zero point energy. The Franck−Condon (FC) factors for the photoionization of C_6H_5NH were calculated using the harmonic approximation for harmonic frequencies and normal modes in the neutral and cationic ground states, as well as the first triplet ionic state, and the Condon approximation for the dipole moment. The Duschinsky effect was considered using recursive formulae

DOI: 10.1021/acs.jpca.9b07273
J. Phys. Chem. A 2019, 123, 9193−9198

already implemented in the Gaussian09 software package. For FC calculations, the rotational and vibrational temperatures were set equal to 300 K.

RESULTS AND DISCUSSION

The 2D coincident signal as a function of electron and photon energy for the anilino radical, that is, filtered on m/z 92, is shown in Figure 2 along with the mass-selected total ion yield (TIY). The ground state of the cation appears to have an onset located at 8.02 ± 0.02 eV. The TIY is reaching a plateau around 8.3 eV, marking the upper limit of the ground state, while upwards from approximately 9.0 eV, the signal becomes noisier, and at slightly higher energies, namely, 9.5 eV, the first excited state of the cation is observed, which slightly contributes to the TIY signal increase above 9.4 eV.

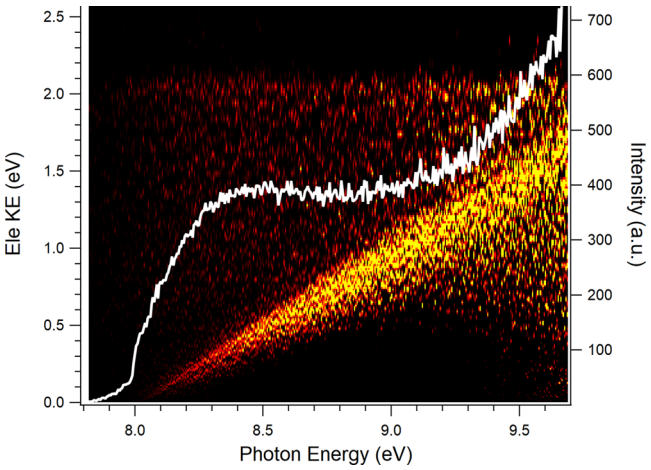

Figure 2. Intensity matrix of the anilino radical (92 amu). The matrix reflects the relative number of counts of electron-ion coincidences recorded as a function of the photon energy (x axis) and the kinetic energy of the photoelectrons (y axis, left). Superimposed in white is the total ion yield, which consists of the accumulated ion signals detected in coincidence as a function of photon energy. Its intensity is displayed on the right y axis in arbitrary units.

The TPES recorded for m/z 92 is shown in Figure 3, along with the theoretical simulation. There are two spectral signatures observed assigned to the $X^{+1}A' \leftarrow X^2A''$ ionizing transition to the ground state of the molecular ion, which is calculated at 8.04 eV, and to the $a^{+3}A'' \leftarrow X^2A''$ transition to the first excited state, calculated at 9.35 eV. The positions of the ground state vibrational bands match well with the calculated spectrum, and we can make out the first five vibrational bands of the cation. The agreement is less satisfactory when comparing relative band ratios, either due to limitations of the Franck−Condon simulation or, as mentioned above, to the presence of autoionization resonances affecting the vibrational branching ratios.[36] The TPES displays one hot band prior to the ionization onset, namely, at 7.96 eV. The presence of hot bands is commonly observed in radicals formed by H abstraction by fluorine atoms since they are always very exothermic in nature due to the formation of a strong H−F bond.[37] Note that this band cannot be explained by the presence of other isomers, which would appear at higher photon energies.

The first adiabatic ionization energy (AIE) is measured to be 8.02 ± 0.02 eV in comparison to the simulated spectrum. The only prior measurement of the vertical ionization energy of the anilino radical was 8.23 ± 0.1 eV and was made by Palmer and Lossing.[13]

It is interesting to compare the AIE of anilino to those of the three possible picolyl structural isomers. Palmer and Lossing[13] already performed a comparison of ionization energies between the four isomers and found that the substitution of CH for N had the largest effect on the para position, that is, for the 4-picolyl radical, which is exactly the opposite of what we observe here. Indeed, the adiabatic ionization energies of anilino and 4-picolyl radicals are the same within the error bars, whereas the 2- and 3-picolyl radicals have noticeably lower IEs. It should be mentioned that Palmer and Lossing employed thermal decomposition of *N*-allylaniline at 870 °C to obtain anilino radicals, so the higher value they obtained could be due to the presence of other isomers. The AIEs of the picolyl isomers have also been recently measured from their recorded TPES by Reusch et al.[27] They rationalized the lower AIE of the 2- and 3-picolyl radicals in terms of charge

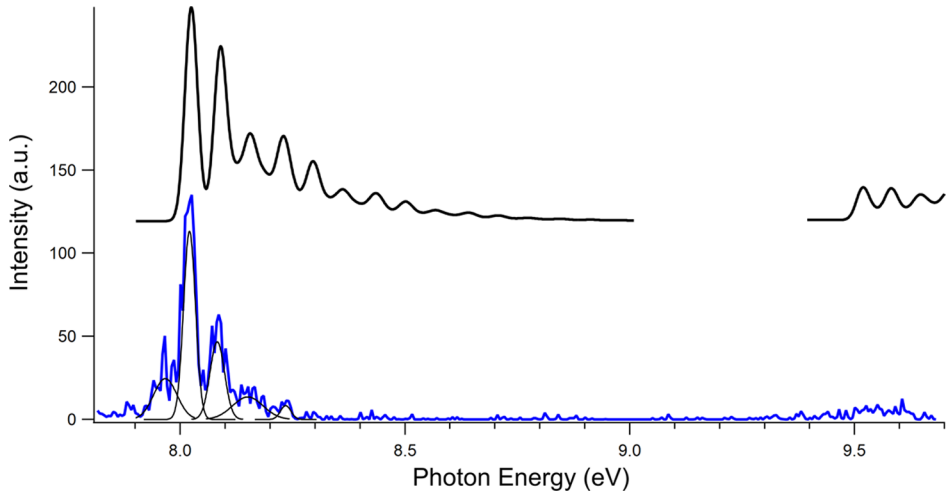

Figure 3. (Blue, bottom) TPES of the anilino radical obtained from the matrix in Figure 2. To guide the eye, superimposed on the TPES are fitted Gaussian peaks. (Black, top) Calculated TPES. The theoretical spectrum of the $a^{+3}A''$ state has been shifted to higher energies by 0.17 eV to match the energy of the experiment, while the theoretical spectrum of the $X^{+1}A'$ state has been shifted to lower energies by 0.02 eV.

DOI: 10.1021/acs.jpca.9b07273
J. Phys. Chem. A 2019, 123, 9193−9198

delocalization: in the case of 4- and 2-picolyl radicals, there is always a resonance structure that places the positive charge in the electrophilic N atom, while there is no such structure for the meta 3-picolyl radical, which confers it more stability in the cation, lowering the ionization energy. The largest positive charge on the N atom was found for the 4-picolyl and was given as the reason for the ∼300 meV shift to a higher ionization energy. As shown in Scheme 1, the anilino radical

Scheme 1. Charge Resonance Structures of Anilino (Top) and 4-Picolyl (Bottom) Radicals

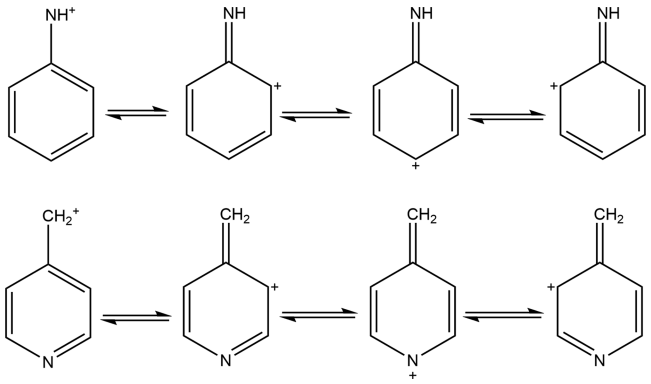

also has a resonance structure where the charge is placed in the N atom, lowering the cation stability and increasing its ionization energy so that it matches that of 4-picolyl.

Comparison of the anilino TPES recorded in this work with the ones reported by Reusch et al.[27] for the picolyl radicals (see Figure S2) shows that the four isomers have similar vibrational progressions (see Table 1), arising solely from the

Table 1. Ionization Energy, Computed Ionization Energy, and the Vibrational Progression of the Anilino Radical in Comparison with Those of the Picolyl Radicals Obtained by Reusch et al.[27]

isomer	ionization energy (eV)	computed values (eV)	ν^+_{exp} (cm^{-1})
anilino	8.02 ± 0.02	8.03	530
4-picolyl	8.01 ± 0.01	8.06	530
3-picolyl	7.59 ± 0.01	7.65	560
2-picolyl	7.70 ± 0.02	7.73	520

in-plane deformation mode of the ring, ν^+_{29}, in line with the geometry changes upon ionization. Indeed, upon ionization of both anilino and picolyl radicals, the most significant bond contraction takes place between the external moieties (−NH and $-CH_2$, respectively) and the aromatic ring (see Table S1 of the Supporting Information for the calculated anilino neutral and cationic geometries). In addition, in all four isomers, the ring atoms undergo a rearrangement that leads to the excitation of the same in-plane deformation mode, ν^+_{29}, as shown in Figure S3 of the Supporting Information for the anilino cation. As was the case for the ionization energies, the mode frequencies are equal within the experimental error bars in the case of anilino and 4-picolyl radicals so that the TPES in the region of the ground cationic state are identical for these two isomers.

Finally, despite a weak intensity signal, the $a^{+3}A''$ excited state is also observed in the TPES. Unfortunately, the signal is nonetheless too weak for any spectroscopic parameters to be extracted from the TPES, and we can only estimate its ionization energy at 9.5 eV.

CONCLUSIONS

We have presented and discussed the threshold photoelectron spectrum of the anilino radical. The anilino radical was produced via hydrogen abstraction of an aniline precursor with fluorine atoms obtained from flowing molecular fluorine through a microwave discharge. The spectrum shows a clear adiabatic transition to the ground state of the cation, with a prominent (0-0) origin band at 8.02 ± 0.02 eV followed by a progression on the in-plane deformation mode, as in the case of the benzyl[38] or picolyl[27] radicals, assigned by comparison with a simulated photoelectron spectrum.

Furthermore, in recent years, coincident techniques combining mass spectrometry and mass-selected PES and TPES fingerprints have been implemented in species identification in complex gas mixtures such as mixed flames due to their multiplexing capabilities and sensitivity to molecular structure, particularly aiming at the structural isomer differentiation.[20−22] The TPES recorded here therefore adds to the increasing database to be used by groups applying PEPICO techniques to identify reactive intermediates. However, we note that the observed similarity between the TPES of anilino and 4-picolyl isomers would require additional information to differentiate them, such as vibronic structures of the cationic excited states, state-selected fragmentation patterns, or an a priori chemical knowledge of the expected species.

ASSOCIATED CONTENT

Supporting Information

The Supporting Information is available free of charge on the ACS Publications website at DOI: 10.1021/acs.jpca.9b07273.

Calculated geometry parameters of the neutral anilino radical and its cation, a TOF spectrum of the products observed during the experiment, a figure displaying the deformation mode ν^+_{29}, and a figure comparing the TPES of the anilino radical and the 4-picolyl radical (PDF)

AUTHOR INFORMATION

Corresponding Author

*E-mail: hrodmarsson@strw.leidenuniv.nl; hr.hrodmarsson@gmail.com. Phone (HRH office): (+33) (0) 1 69 35 99 50.

ORCID

Helgi Rafn Hrodmarsson: 0000-0002-9613-5684
Gustavo A. Garcia: 0000-0003-2915-2553
Bérenger Gans: 0000-0001-9658-2436

Present Address

#Sackler Laboratory for Astrophysics, Leiden Observatory, Leiden University, P.O. Box 9513, NL-2300 RA Leiden, The Netherlands.

Notes

The authors declare no competing financial interest.

ACKNOWLEDGMENTS

We are grateful to the whole SOLEIL for provision of synchrotron radiation under proposal number 99180002 and J.-F. Gil for his technical assistance on the SAPHIRS end-station. This work received financial support from the French Agence Nationale de la Recherche (ANR) under grant ANR-12-BS08-0020-02 (project SYNCHROKIN).

DOI: 10.1021/acs.jpca.9b07273
J. Phys. Chem. A 2019, 123, 9193−9198

REFERENCES

(1) Roberts, G. M.; Stavros, V. G. The role of $\pi\sigma^*$ states in the photochemistry of heteroaromatic biomolecules and their subunits: insights from gas-phase femtosecond spectroscopy. *Chem. Sci.* **2014**, *5*, 1698−1722.

(2) Ashfold, M. N.; Cronin, B.; Devine, A. L.; Dixon, R. N.; Nix, M. G. The role of $\pi\sigma^*$ excited states in the photodissociation of heteroaromatic molecules. *Science* **2006**, *312*, 1637−1640.

(3) Sobolewski, A. L.; Domcke, W.; Dedonder-Lardeux, C.; Jouvet, C. Excited-state hydrogen detachment and hydrogen transfer driven by repulsive $1\pi\sigma^*$ states: A new paradigm for nonradiative decay in aromatic biomolecules. *Phys. Chem. Chem. Phys.* **2002**, *4*, 1093−1100.

(4) Ray, J.; Ramesh, S. G. Conical intersections involving the lowest $^1\pi\sigma^*$ state in aniline: Role of the NH_2 group. *Chem. Phys.* **2018**, *515*, 77−87.

(5) Kohse-Höinghaus, K.; Oßwald, P.; Cool, T. A.; Kasper, T.; Hansen, N.; Qi, F.; Westbrook, C. K.; Westmoreland, P. R. Biofuel Combustion Chemistry: From Ethanol to Biodiesel. *Angew. Chem., Int. Ed.* **2010**, *49*, 3572−3597.

(6) Glarborg, P.; Jensen, A. D.; Johnsson, J. E. Fuel nitrogen conversion in solid fuel fired systems. *Prog. Energy Combust. Sci.* **2003**, *29*, 89−113.

(7) Parker, D. S. N.; Kaiser, R. I. On the formation of nitrogen-substituted polycyclic aromatic hydrocarbons (NPAHs) in circumstellar and interstellar environments. *Chem. Soc. Rev.* **2017**, *46*, 452−463.

(8) King, G. A.; Oliver, T. A. A.; Ashfold, M. N. R. Dynamical insights into $^1\pi\sigma^*$ state mediated photodissociation of aniline. *J. Chem. Phys.* **2010**, *132*, 214307.

(9) Balucani, N., Pacifici, L., Skouteris, D., Caracciolo, A., Casavecchia, P., Falcinelli, S., Rosi, M. A Computational Study of the Reaction $N(^2D) + C_6H_6$ Leading to Pyridine and Phenylnitrene. In *Computational Science and Its Applications - ICCSA 2018*; 1st ed.; Misra, S., Ed. Springer International Publishing, 2019.

(10) Balucani, N., Pacifici, L., Skouteris, D., Caracciolo, A., Casavecchia, P., Falcinelli, S., Rosi, M. A Theoretical Investigation of the Reaction $N(^2D) + C_6H_6$ and Implications for the Upper Atmosphere of Titan. In *Computational Science and Its Applications - ICCSA 2018*; 1st ed.; Misra, S., Ed. Springer International Publishing, 2019.

(11) Porter, G.; Wright, F. J. Primary Photochemical Processes in Aromatic Molecules. Part 3. Absorption Spectra of Benzyl, Anilino, Phenoxy and Related Free Radicals. *Trans. Faraday Soc.* **1955**, *51*, 1469.

(12) Norman, I.; Porter, G. Trapped Atoms and Radicals in Rigid Solvents. *Proc R. Soc. London Ser. −Math. Phys. Sci.* **1955**, *230*, 399.

(13) Palmer, T. F.; Lossing, F. P. Free Radicals by Mass Spectrometry. XXX. Ionization Potentials of Anilino and 2-, 3- and 4-Pyridylmethyl Radicals. *J. Am. Chem. Soc.* **1963**, *85*, 1733.

(14) Land, E. J.; Porter, G. Primary Photochemical Processes in Aromatic Molecules. Part 8. —Absorption Spectra and Acidity Constants of Anilino Radicals. *Trans. Faraday Soc.* **1963**, *59*, 2027.

(15) McMillen, D. F.; Golden, D. M. Hydrocarbon Bond Dissociation Energies. *Annu. Rev. Phys. Chem.* **1982**, *33*, 493−532.

(16) Drzaic, P. S.; Brauman, J. I. Electron Photodetachment from Phenylnitrene, Anilide, and Benzyl Anions - Electron-Affinities of the Anilino and Benzyl Radicals and Phenylnitrene. *J. Phys. Chem.* **1984**, *88*, 5285−5290.

(17) Tripathi, G. N. R.; Schuler, R. H. Time Resolved Resonance Raman Spectra of Anilino Radical and Aniline Radical Cation. *J. Chem. Phys.* **1987**, *86*, 3795−3800.

(18) Wren, S. W.; Vogelhuber, K. M.; Ichino, T.; Stanton, J. F.; Lineberger, W. C. Photoelectron Spectroscopy of Anilinide and Acidity of Aniline. *J. Phys. Chem. A* **2012**, *116*, 3118−3123.

(19) Baer, T.; Tuckett, R. P. Advances in threshold photoelectron spectroscopy (TPES) and threshold photoelectron photoion coincidence (TPEPICO). *Phys. Chem. Chem. Phys.* **2017**, *19*, 9698−9723.

(20) Krüger, J.; Garcia, G. A.; Felsmann, D.; Moshammer, K.; Lackner, A.; Brockhinke, A.; Nahon, L.; Kohse-Höinghaus, K. Photoelectron-photoion coincidence spectroscopy for multiplexed detection of intermediate species in a flame. *Phys. Chem. Chem. Phys.* **2014**, *16*, 22791−804.

(21) Felsmann, D.; Lucassen, A.; Krüger, J.; Hemken, C.; Tran, L.-S.; Pieper, J.; Garcia, G. A.; Brockhinke, A.; Nahon, L.; Kohse-Höinghaus, K. Progress in Fixed-Photon-Energy Time-Efficient Double Imaging Photoelectron/Photoion Coincidence Measurements in Quantitative Flame Analysis. *Z. Phys. Chem.* **2016**, *230*, 1067−1097.

(22) Pieper, J.; Schmitt, S.; Hemken, C.; Davies, E.; Wullenkord, J.; Brockhinke, A.; Krüger, J.; Garcia, G. A.; Nahon, L.; Lucassen, A.; Kohse-Höinghaus, K. Isomer Identification in Flames with Double-Imaging Photoelectron/Photoion Coincidence Spectroscopy (i^2PEPICO) using Measured and Calculated Reference Photoelectron Spectra. *Z. Phys. Chem.* **2018**, *232*, 153−187.

(23) Bodi, A.; Hemberger, P.; Osborn, D. L.; Sztáray, B. Mass-Resolved Isomer-Selective Chemical Analysis with Imaging Photoelectron Photoion Coincidence Spectroscopy. *J. Phys. Chem. Lett.* **2013**, *4*, 2948−2952.

(24) Oßwald, P.; Hemberger, P.; Bierkandt, T.; Akyildiz, E.; Köhler, M.; Bodi, A.; Gerber, T.; Kasper, T. In situ flame chemistry tracing by imaging photoelectron photoion coincidence spectroscopy. *Rev. Sci. Instrum.* **2014**, *85*, No. 025101.

(25) Cunha de Miranda, B.; Garcia, G. A.; Gaie-Levrel, F.; Mahjoub, A.; Gautier, T.; Fleury, B.; Nahon, L.; Pernot, P.; Carrasco, N. Molecular Isomer Identification of Titan's Tholins Organic Aerosols by Photoelectron/Photoion Coincidence Spectroscopy Coupled to VUV Synchrotron Radiation. *J. Phys. Chem. A* **2016**, *120*, 6529−40.

(26) Baeza-Romero, M. T.; Gaie-Levrel, F.; Mahjoub, A.; López-Arza, V.; Garcia, G. A.; Nahon, L. A smog chamber study coupling a photoionization aerosol electron/ion spectrometer to VUV synchrotron radiation: organic and inorganic-organic mixed aerosol analysis. *Eur. Phys. J. D* **2016**, *70*, 154.

(27) Reusch, E.; Holzmeier, F.; Constantinidis, P.; Hemberger, P.; Fischer, I. Isomer-Selective Generation and Spectroscopic Characterization of Picolyl Radicals. *Angew. Chem., Int. Edit.* **2017**, *56*, 8000−8003.

(28) Nahon, L.; de Oliveira, N.; Garcia, G. A.; Gil, J. F.; Pilette, B.; Marcouillé, O.; Lagarde, B.; Polack, F. DESIRS: a state-of-the-art VUV beamline featuring high resolution and variable polarization for spectroscopy and dichroism at SOLEIL. *J. Synchroton. Radiat.* **2012**, *19*, 508−520.

(29) Garcia, G. A.; Tang, X.; Gil, J.-F.; Nahon, L.; Ward, M.; Batut, S.; Fittschen, C.; Taatjes, C. A.; Osborn, D. L.; Loison, J.-C. Synchrotron-based double imaging photoelectron/photoion coincidence spectroscopy of radicals produced in a flow tube: OH and OD. *J. Chem. Phys.* **2015**, *142*, 164201.

(30) Tang, X.; Garcia, G. A.; Gil, J.-F.; Nahon, L. Vacuum upgrade and enhanced performances of the double imaging electron/ion coincidence end-station at the vacuum ultraviolet beamline DESIRS. *Rev. Sci. Instrum.* **2015**, *86*, 123108.

(31) Garcia, G. A.; Cunha de Miranda, B. K.; Tia, M.; Daly, S.; Nahon, L. DELICIOUS III: A multipurpose double imaging particle coincidence spectrometer for gas phase vacuum ultraviolet photodynamics studies. *Rev. Sci. Instrum.* **2013**, *84*, No. 053112.

(32) Garcia, G. A.; Nahon, L.; Powis, I. Two-dimensional charged particle image inversion using a polar basis function expansion. *Rev. Sci. Instrum.* **2004**, *75*, 4989−4996.

(33) Briant, M.; Poisson, L.; Hochlaf, M.; de Pujo, P.; Gaveau, M. A.; Soep, B. Ar_2 Photoelectron Spectroscopy Mediated by Autoionizing States. *Phys. Rev. Lett.* **2012**, *109*, 193401.

(34) Frisch, M. J.; Trucks, G. W.; Schlegel, H. B.; Scuseria, G. E.; Robb, M. A.; Cheeseman, J. R.; Scalmani, G.; Barone, V.; Mennucci, B.; Petersson, G. A. et al. *Gaussian 09*; Gaussian Inc.: Wallingford, CT, 2009.

(35) Williams, R. L.; Rowland, F. S. Hydrogen-Atom Abstraction by Fluorine Atoms. *J. Phys. Chem.* **1973**, *77*, 301−307.

DOI: 10.1021/acs.jpca.9b07273
J. Phys. Chem. A 2019, 123, 9193−9198

(36) Hager, J.; Smith, M. A.; Wallace, S. C. Autoionizing Rydberg Structure Observed in the Vibrationally Selective, two-color, Threshold Photoionization Spectrum of Jet-Cooled Aniline. *J. Chem. Phys.* **1985**, *83*, 4820−4822.
(37) Baer, T.; Guyon, P.-M., An Historical Introduction to Threshold Photoionization. In *High Resolution Laser Photoionization and Photoelectron Studies*; Powis, I.; Baer, T.; Ng, C.-Y. Ed. John Wiley & Sons: Chichester, U.K., 1995; p 1.
(38) Savee, J. D.; Zádor, J.; Hemberger, P.; Sztáray, B.; Bodi, A.; Osborn, D. L. Threshold photoelectron spectrum of the benzyl radical. *Mol. Phys.* **2014**, *113*, 2217−2227.

DOI: 10.1021/acs.jpca.9b07273
J. Phys. Chem. A 2019, 123, 9193−9198